

Orbitally degenerate spin-fluctuation model for heavy-fermion superconductivity

M. R. Norman

Materials Science Division, Argonne National Laboratory, Argonne, Illinois 60439

(Received 3 March 1994; revised manuscript received 14 April 1994)

In this paper, a generalization of standard spin-fluctuation theory is considered by replacing the simple Hubbard interaction by the screened Hartree-Fock interaction for f electrons. This model is then used in both an LS and a JJ coupling scheme to construct the particle-particle scattering vertex. In an on-site approximation, this vertex is shown to lead to an instability for a superconducting pair state which obeys Hund's rules, with $L=5$, $S=1$, and $J=4$, whereas for near-neighbor pairing, the most attractive instability is for $J=0$. The degeneracy of these multiplets is broken by anisotropy of the quasiparticle wave functions. Detailed calculations are presented for the case of UPt_3 .

I. INTRODUCTION

After over a decade's worth of theoretical work, there is no overall agreement on a microscopic theory for heavy-fermion superconductivity. The overall prejudice, though, is that the underlying pairing mechanism is similar to that operative in superfluid ^3He . Most attempts at a theory based on this approach have been to make the simplest possible modifications to the standard single-orbital Hubbard interaction used in the ^3He problem. These attempts have had mixed success. The philosophy of this paper will be to actually do for heavy fermions what was done for ^3He , that is, to use the Hartree-Fock interaction between f electrons including full orbital and spin-orbital effects and construct the effective particle-particle vertex by the appropriate diagrammatic summation. In principle, this theory contains all relevant physics within a spin-fluctuation-based approach. Even at the simplest level, new physics emerges which is not present when using a simple Hubbard interaction. In particular, for on-site pairing, the maximum instability in the particle-particle vertex occurs for a pair state which obeys Hund's rules. For f electrons, this corresponds to a state which has $L=5$, $S=1$, and $J=4$. The degeneracy of this multiplet is broken in real metals by crystalline anisotropy effects in the normal state. This is reflected by (1) the orbital and momentum dependence of the bare susceptibility bubble which forms the internal lines of the vertex and (2) the orbital and momentum dependence of the quasiparticle wave functions which form the external lines. In this paper, (1) is treated in a simple manner and (2) is treated within a band-theoretic approximation. The frequency dependence of (1) and (2), which acts to set the overall scale for T_c , is also treated in a simple fashion. The theory has the advantage that it can be systematically improved by removing these approximations. The above ideas are illustrated by calculations for UPt_3 .

In the second section, a motivation of this theory is given by looking at some systematics of heavy-fermion superconductors and by comparing the heavy-fermion problem to that of ^3He . In the third section, the general formalism is described. The single-orbital version of this theory is shown to yield the paramagnon model for ^3He .

The standard spin-fluctuation models worked on previously are then shown to be a lattice generalization of the single-orbital model. In the fourth section, the formalism for the f -electron problem is derived, with the particle-particle vertex equations solved for various approximations for the susceptibility bubble in both an LS and a JJ coupling scheme. General properties of the vertex are described based on group theory. In the fifth section, the pair vertex is projected onto the Fermi surface. Calculations are then described for the case of UPt_3 , utilizing information from a relativistic band-structure calculation. In the last section, future directions, including the question of intersite pairing effects, will be discussed. A shorter version of this work has appeared earlier.¹

II. BACKGROUND

Sufficient evidence has accumulated over the past 11 years to demonstrate that the superconductivity seen in a number of f -electron metals with large effective mass is unconventional in nature, that is, the group representation describing the order parameter is almost certainly not the identity representation (Γ_1^+). This, along with a variety of other facts, casts doubt on a traditional electron-phonon mechanism as mediating the pairing. The first theoretical work in this area ten years ago showed a close connection of these metals with superfluid ^3He .² In particular, they are near both a magnetic and a localization instability. A classic example is UPt_3 . Doping with Pd, for instance, causes this metal to become strongly antiferromagnetic. Further doping causes the f electrons to become localized.³ Anderson² also emphasized that the on-site part of the interaction must be playing a major role given the large ratio (~ 0.1) of the superconducting transition temperature to the Fermi energy. This important observation has been largely ignored. Anderson⁴ was also the first to point out that heavy-fermion superconductors have two f atoms per unit cell. For on-site pairing, one can have an odd-parity ground state in this case (with one atom per cell, the pair state would have to be even for on-site pairing). This unusual observation has also been largely ignored, except in a later paper by Appel and Hertel⁵ where a formalism

for describing localized pairs for UPt_3 was developed in great detail. The reason the above points were largely ignored was the observation of antiferromagnetic spin fluctuations in several heavy-fermion superconductors by neutron scattering.⁶ Such fluctuations occur because of exchange interactions between near-neighbor sites. This led to a picture of near-neighbor pairing based on these fluctuations by a number of authors.^{7,8} Subsequent work largely concentrated on generalizing these simple theories to handle the nonsymmorphic (hcp) lattice structure of UPt_3 .^{9,10} These theories have had mixed success. In particular, available data on UPt_3 point to a pair state from a two-dimensional group representation with both line and point nodes and probably of odd parity.^{11,12} This state would have $\Gamma_6^- (E_{2u})$ symmetry. Although nontrivial group representations occur in these calculations, this particular state has never emerged as the ground state. The last work done in this area by the author¹³ indicated that the anisotropy of the quasiparticle wave functions plays a fundamental role because this problem cannot be reduced to an effective one-band form given the two f atoms per unit cell. Therefore these earlier single-band models are most likely inadequate for describing real heavy-fermion metals. Moreover, the orbital degeneracy of the f electrons, particularly in the uranium case, also brings into question any single-orbital treatment of the problem.

This paper is an attempt to improve on these earlier theories by explicitly including multiorbital effects. This work was motivated by several additional issues than those listed above. A number of alternate theories have been proposed recently, in particular by Cox¹⁴ and by Coleman, Miranda, and Tsvetlik,¹⁵ which emphasize an on-site pairing viewpoint. Cox's work is important in that he emphasized the important role that orbital effects play in this problem. Another key motivation was an experiment by Osborn *et al.*¹⁶ which detected excitations between Coulomb multiplets with high-energy neutron scattering, not only in localized f metals like Pr and UPd_3 , but also in UPt_3 itself. This indicates that multiplet correlations present in atoms survive even in a metal with itinerant f quasiparticles. In Table I, the seven known heavy-fermion superconductors are listed. There are two striking things about this table. First, six of the seven are uranium alloys. Moreover, there is strong ex-

TABLE I. List of known heavy-fermion superconductors with the number of f atoms per unit cell. In parentheses is the nature of the low-temperature distorted phase in the single- f -atom case (QP, quadrupolar; AF, antiferromagnetic; ?, not fully determined) and the resulting number of f atoms.

Case	f atoms
UPt_3	2
UBe_{13}	2
U_2PtC_2	2
URu_2Si_2	1 (QP/AF—2)
UPd_2Al_3	1 (AF—2)
UNi_2Al_3	1 (AF—2)
CeCu_2Si_2	1 (?—2?)

perimental evidence that the uranium atoms are close to an f^2 configuration. The magnetic susceptibilities of UPt_3 (Ref. 3) and UPd_2Al_3 (Ref. 17) look almost identical to that of the local f^2 metal PrNi_5 .¹⁸ The susceptibility of URu_2Si_2 has been most successfully explained based on an f^2 ground state.¹⁹ Cox's quadrupolar model²⁰ for UBe_{13} is also based on an f^2 configuration. It should also be noted that UPt_3 is very similar to UPd_3 (similar crystal structures, almost identical f -atom separations) yet the latter is clearly a local f^2 metal.²¹ In the high-energy neutron data,¹⁶ the Coulomb excitation seen in these two metals looks very similar. This would be hard to imagine if UPt_3 was not close to being f^2 . As for CeCu_2Si_2 , it may not be like the rest, although it has been pointed out that an f^2 admixture is needed to explain its properties with the Anderson impurity model.²² The importance of these facts is that since the f atom has two bare f electrons per site, this leads to a strong motivation that the superconducting pairs have two f quasiparticles per site from a trial wave function point of view. The second striking point of Table I is that all of these metals either have two f atoms per unit cell, or undergo some sort of magnetic transition at temperatures above the superconducting transition which gives a new unit cell with two f atoms. As discussed above, this fact has little relevance to a near-neighbor pairing model (since an atom in any crystal structure has near neighbors), but plays a crucial role for on-site pairing (since one can have even-parity or odd-parity pairing depending on the relative sign of the order parameter on the two sites).

A further motivation of the importance of on-site pairing can be obtained by comparing the case of ^3He to uranium alloys. In Fig. 1, a plot is shown of the interaction potential of two He atoms.²³ This is similar to what one would expect of two f electrons on a uranium site. In particular, there is strong repulsion at small interparti-

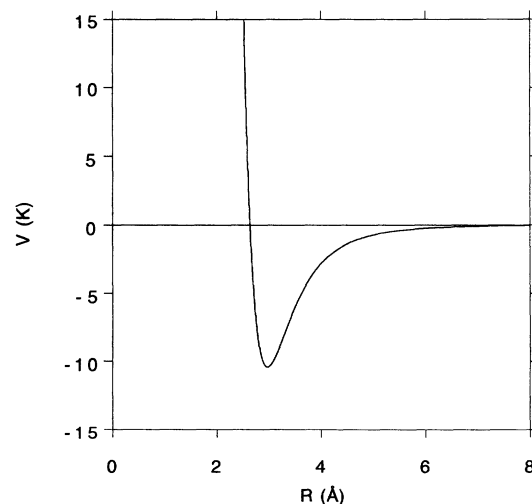


FIG. 1. Interaction potential between two He atoms (Ref. 23). The interaction potential of two f electrons of a uranium ion would look similar with appropriately scaled axes (attraction in that case is due to the ion core, though, which is technically a three-body effect).

cle separation due to the Coulomb repulsion between the two f electrons, there is attraction at intermediate distances (of order 3 a.u.) since the ion-core attraction exceeds this repulsion in this range (which leads to an f^2 ground state), and then the potential weakens at large separation due to the exponential decay of the f -electron radial function. This analogy should not be taken too far, though, since the source of attraction in the helium case is the van der Waals force, whereas in the current case the attraction is provided by the ion core, which is technically a three-body effect. Also, the direct interaction potential for ${}^3\text{He}$ has been shown to be inadequate for describing the pairing of He atoms in the superfluid state (it predicts $L=2$ pairing).²⁴ The reason for this is the major role that collective effects play due to polarization of the medium.²⁵⁻²⁹ This led to the development of the paramagnon model for ${}^3\text{He}$. In this model, a much simpler direct interaction potential is used, a repulsive contact interaction between atoms of opposite spin (i.e., the bare attraction is not included). But this potential in turn is used to sum a diagrammatic series to all orders, thus including the important collective effects. This gives a good description of the superfluid state of ${}^3\text{He}$.^{27,30} In this paper, a similar approach is taken to the current problem, with a generalization considered which includes multiorbital effects necessary in dealing with f electrons. The paramagnon model for ${}^3\text{He}$, as well as previous spin-fluctuation models for heavy fermions, are subsets of this more general theory.

III. GENERAL FORMALISM

The particle-particle vertex is defined by

$$\Gamma^{abcd} = \Gamma_0^{abcd} - \sum_{e,f} \Gamma_0^{aecf} \chi_0^{ef} \Gamma^{fbed}, \quad (1)$$

where Γ_0 is the bare vertex, χ_0 is the bare susceptibility bubble, the indices label orbitals, and the minus sign is due to the closed fermion loop defining the bubble (in Γ , the first two indices label incoming lines, the last two outgoing lines). Γ_0 is taken to be the antisymmetrized Coulomb interaction ($V^{abcd} - V^{abdc}$)

$$\Gamma_0^{abcd} = \sum_k c_k^{abcd} F_k, \quad (2)$$

where c_k are combinations of $3j$ symbols and F_k are Coulomb multipole (Slater) integrals defined on p. 217 of Ref. 31. (A simpler expression of this type has been used in earlier spin-fluctuation work³² and in an Anderson model approach.³³) For s electrons, Eq. (2) reduces to

$$\Gamma_0^{abcd} = \delta_{ac} \delta_{bd} - \delta_{ad} \delta_{bc} \equiv \frac{1}{2} (\delta_{ac} \delta_{bd} - \sigma_{ac} \cdot \sigma_{bd}), \quad (3)$$

where the last term is a scalar product of Pauli spin matrices and the indices now label just spins (1 for up, 2 for down). Equation (1) is easily solved, giving^{27,28}

$$\Gamma^{1111} = -F_0^2 \chi_0 / (1 - F_0^2 \chi_0^2), \quad (4)$$

$$\Gamma^{1212} = F_0 + F_0^3 \chi_0^2 / (1 - F_0^2 \chi_0^2). \quad (5)$$

Equation (4) [5] is a sum of odd (even) number of longitudinal ($e=f$) bubbles. The triplet ($S=1$) vertex is just Eq. (4), the singlet ($S=0$) vertex is $2\Gamma^{1212} - \Gamma^{1111}$ (since Γ^{1212} is half the sum of the singlet and triplet vertices²⁷). Alternately, the singlet vertex is $\Gamma^{1212} - \Gamma^{1221}$ [i.e., antisymmetrizing Eq. (5)] where the latter term is a sum of transverse ($e \neq f$) bubbles (i.e., ladder diagrams). These expressions are equivalent of course. Equations (4) and (5) form the basis of the standard paramagnon model (where F_0 is generally denoted as I).

The first thing to note from the above is that the triplet vertex is negative (attractive) and the singlet one positive (repulsive). Thus, the vertex exhibits Hund's first rule (maximal S). In the ${}^3\text{He}$ problem, the L of the pair state is determined by projecting Eq. (4) onto the Fermi surface. Since it is isotropic, and L must be odd (since $S=1$), it is necessary to include the momentum dependence of χ_0 to obtain a nonzero projection. As expected, $L=1$ is found since this function has the largest projection on a spherical Fermi surface for odd- L harmonics. Note that the momentum dependence is not critical, it is only necessary to give a nonzero projection. In fact, very different models of the momentum dependence of the vertex give identical pairing coupling constants.³⁴ A physical picture of the pairing in these models based on mutual interaction of the two particles via their polarization clouds (a generalized Zeeman effect) has been given by Leggett.²⁹

This picture can be contrasted with that given for the heavy fermions and high- T_c cuprates based on singlet ($L=2$) pairing.⁷ This "violation" of Hund's rules is obtained by considering pairing of electrons on near-neighbor atoms in a nearly antiferromagnetic metal. In such a case, $\chi(\mathbf{Q}) > \chi(0)$, where \mathbf{Q} is the ordering wave vector (assumed to be commensurate with the lattice corresponding in real space to antialignment of near-neighbor spins) and χ is the dressed bubble. This means in real space that $\chi(R, R')$ is negative (R, R' are site indices, with R' a near neighbor of R). This can be achieved by having momentum dependence in either χ_0 or in Γ_0 [χ being defined by an equation similar to Eq. (1)]. The latter is preferable, in that commensurate \mathbf{Q} are rarely obtained for χ_0 except in special circumstances, and has been used for fitting neutron scattering data both in heavy fermions⁶ and in high- T_c cuprates.³⁵ Now, the same thing which gives a negative $\chi(R, R')$ also gives a sign for $\Gamma(R, R', R, R')$ opposite to that of $\Gamma(R, R, R, R)$. Therefore, if the order parameter is such that $\Delta(R, R)$ is zero and $\Delta(R, R')$ is nonzero (such as found for certain d -wave states), then one can have $S=0$ pairing. Note the complete difference in physics than that discussed above for the ${}^3\text{He}$ problem. In particular, the momentum dependence is crucial for this argument. From the lattice point of view, ${}^3\text{He}$ is actually more closely related to on-site pairing models than to near-neighbor pairing models.

IV. f ELECTRONS

The formalism of the previous section is now applied to the problem of f electrons. At the bare interaction level, we are already faced with the problem that the uranium

ion is in the intermediate-coupling regime (i.e., midway between LS and JJ coupling).³⁶ On the other hand, the spin-orbit interaction is large enough that in electronic structure calculations, no $j = \frac{7}{2}$ quasiparticles are occupied.³⁷ Because of this, the susceptibility bubble χ_0 will be almost pure $j = \frac{5}{2}$ in character. Therefore, even if the bare interaction is in the intermediate-coupling regime, the effective interaction for quasiparticles which comes out of Eq. (1) will be in the JJ -coupling limit. Despite this, we will start out by deriving results in the LS -coupling limit to make connections to the ${}^3\text{He}$ problem discussed in the last section. Then, we will turn to the JJ scheme.

We start by reviewing the multiplet structure of the f^2 uranium ion, shown in Fig. 2.³⁶ There are three spin triplets ($L = 1, 3, 5$, each spin-orbit split into three J multiplets) and four spin singlets ($L = 0, 2, 4, 6$). This level structure can be fitted by the following scheme. At the Hartree-Fock level, only Slater integrals of even rank appear. Fits of the spectra can be achieved by reducing these integrals on average by 38%. This effect is due to screening caused by Coulomb correlations (i.e., the particles try to avoid one another, thus reducing their effective interaction) which can be approximately calculated within a configurational interaction (CI) scheme. In addition, CI causes effective operators of odd rank to appear not present at the Hartree-Fock level (known as Trees parameters). These terms are rather small, though, and we ignore them. To discuss the level scheme, it is useful to find linear combinations of the c_k coefficients of Eq. (2) which more clearly reflect the group-theoretical structure of the f electrons, which are labeled e_k . This has been achieved by Racah^{38,39,31} and is equivalent to replacing the Slater integrals F_k ($k = 0, 2, 4, 6$) by linear combinations E_k ($k = 0, 1, 2, 3$). E_0 is defined such that all f^2 terms have this energy ($e_0 = 1$). It is equal to F_0 plus a linear combination of the other F_k terms and is equivalent to the Hubbard U parameter (the other E_k parameters do not contain F_0). E_1 is defined so as to distin-

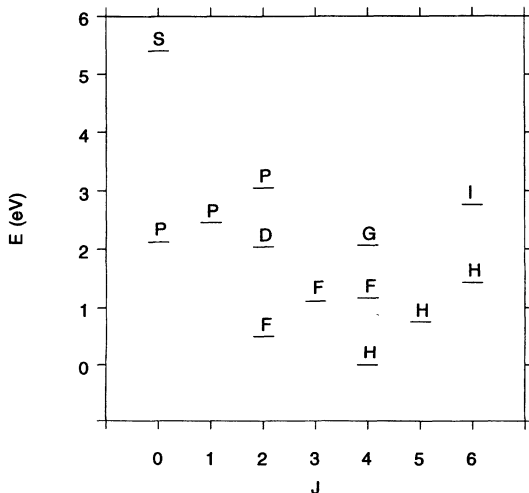


FIG. 2. f^2 multiplet structure of a U^{4+} ion (Refs. 36,83). Energy is plotted versus J , with labels referring to L .

guish spin singlets from spin triplets, with $e_1 = 0$ for triplets and $e_1 = 2$ for all singlets but $L = 0$. Note that these coefficients are identical to the s -electron problem of the previous section. Thus E_1 plays the same role in the f -electron problem as the paramagnon $I(F_0)$ plays in the ${}^3\text{He}$ problem. This is quite interesting, since E_1 is a shape-fluctuation term instead of a charge-fluctuation term (i.e., it does not involve F_0). This means that the inclusion of orbital degeneracy qualitatively changes the physics relative to single-orbital models. As for the $L = 0$ singlet, it has $e_1 = 9$. This is another consequence of orbital degeneracy; basically $L = 0$ has a different group structure than $L = 2, 4, 6$ since it already appears at the f^0 level (i.e., it has a different “quasispin” or “seniority”). We summarize by writing down the expression for e_1 :

$$e_1 = \langle LS | q_{12} | \frac{1}{2} - 2s_1 \cdot s_2 | LS \rangle = 2 - S(S+1) + 7\delta_{L0}, \quad (6)$$

where 1,2 label the two electrons, q is the seniority operator, and s is the spin operator. Note the similarity to the last expression of Eq. (3). As for e_2 , it is isomorphic to $L = 2, 4, 6$ and thus acts to split these three multiplets apart (it is zero for all other L states). The expression for this term is quite complicated and will not be written down. The most interesting parameter is E_3 . It acts to split apart the three spin triplets, with $e_3 = -9, 0, 33$ for $L = 5, 3, 1$ respectively (it is nonzero for all terms but $L = 0$). This can be written as

$$e_3 = [\frac{1}{2} - S(S+1)][L(L+1) - 24g(U)], \quad (7)$$

where $g(U)$ is the Casimir operator of the group G_2 with U labeling the representation of G_2 appropriate for a particular LS state [note that $L(L+1)$ is the Casimir operator for the group SO_3]. The interest is that this has similarities to the case of p electrons, where Van Vleck⁴⁰ showed long ago that the interaction between two p electrons can be written as

$$w_{12} = F_0 + (-5 - 3I_1 \cdot I_2 - 12s_1 \cdot s_2)F_2, \quad (8)$$

with I the orbital angular momentum operator. This looks like an orbital generalization of the last expression in Eq. (3). A summary of the e_k coefficients for the f^2 states is given in Table II.

We now turn to a solution of Eq. (1). At this time, we will assume that $\chi_0^f(\mathbf{q}) = \chi_0$ (i.e., no orbital and momentum dependence to the bubble). This approximation will

TABLE II. f^2 energies in the LS scheme (Ref. 38).

Term	Energy
3H	$E_0 - 9E_3$
3F	E_0
3P	$E_0 + 33E_3$
1I	$E_0 + 2E_1 + 70E_2 + 7E_3$
1G	$E_0 + 2E_1 - 260E_2 - 4E_3$
1D	$E_0 + 2E_1 + 286E_2 - 11E_3$
1S	$E_0 + 9E_1$

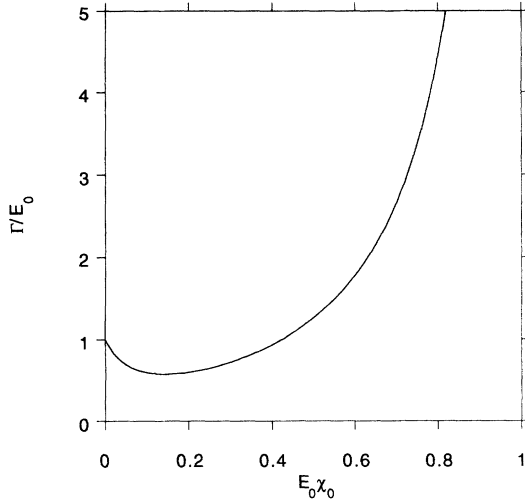


FIG. 3. Effective interaction of Eq. (10) versus χ_0 .

be discussed below. States of definite LS have antisymmetrized wave functions. So the vertex for the state $L=5, M_L=5 (S=1, M_S=1)$ will be

$$\Gamma_{5,5} = \Gamma^{3232} - \Gamma^{3223} - \Gamma_0^{3232}, \quad (9)$$

where indices label m_l (with all spins up). The first term involves longitudinal bubbles, the second transverse bubbles, and the last compensates for double counting (since the bare vertex is antisymmetric by definition). Vertices for other LS states can be obtained either by using the appropriate antisymmetric combination of the Γ or by employing Slater's diagonal sum rule.³¹ This is equivalent to the two derivations of the singlet vertex in the paramagnon model discussed after Eq. (5).

In certain cases, analytic results can be derived by expanding Eq. (1) into a bubble summation, just as was done in the previous section for ^3He . In particular, let us start with just including the E_0 term. The result for all states of definite LS is

$$\Gamma = E_0 / [(1 - E_0\chi_0)(1 + 13E_0\chi_0)] + E_0^2\chi_0 / (1 - E_0\chi_0). \quad (10)$$

The first term comes from longitudinal bubbles, the

$$\Gamma = (4E_1 + 13E_1^2\chi_0 - 126E_1^3\chi_0^2 - 162E_1^4\chi_0^3) / [(1 - 81E_1^2\chi_0^2)(1 - 4E_1^2\chi_0^2)] - 2E_1, \quad (12)$$

where the first term comes from longitudinal bubbles, the second from transverse bubbles, and the third from double counting. Just as for the singlet vertex in ^3He , this interaction, plotted in Fig. 4, is repulsive for $\chi_0=0$ (equal to $2E_1$) and has a positive divergence at $9E_1\chi_0=1$. This expression is also valid for the $L=2$ and $L=4$ singlets. The vertex for the $L=0$ state is more repulsive.

The general solution to Eq. (1) is difficult to construct

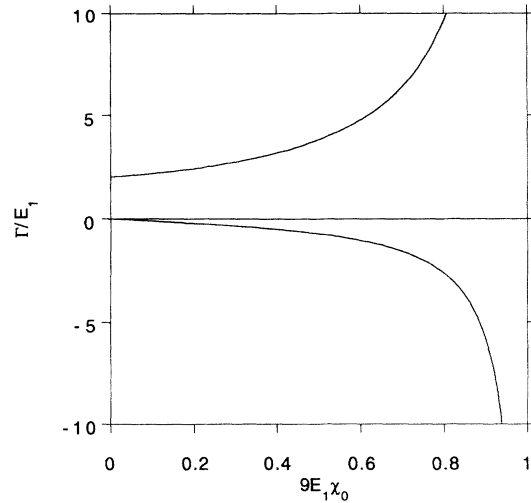


FIG. 4. Effective interaction of Eq. (11) (triplet, lower curve) and Eq. (12) (singlet, upper curve) versus χ_0 . This is very similar to the effective interaction in the ^3He problem.

second from transverse bubbles and double counting. Note that 13 is the orbital degeneracy (14) minus 1. This expression, plotted in Fig. 3, is always repulsive. The behavior of this term is that, as χ_0 increases from zero, the repulsion is reduced compared to E_0 and then begins to increase again and diverges at $E_0\chi_0=1$. This corresponds to a localization instability.

Now assume that only E_1 is nonzero. Analytic results can also be obtained. For the spin-triplet states, Eq. (1) is now

$$\Gamma = -11E_1^2\chi_0 / [(1 - 81E_1^2\chi_0^2)(1 - 4E_1^2\chi_0^2)] + 2E_1^2\chi_0 / (1 - 4E_1^2\chi_0^2), \quad (11)$$

where the first term comes from longitudinal bubbles, and the second from transverse bubbles. This expression, plotted in Fig. 4, is zero for $\chi_0=0$ and then has a negative divergence as $9E_1\chi_0$ approaches 1, corresponding to a magnetic instability. This behavior is analogous to the triplet vertex in ^3He . Equation (1) can also be solved for the $L=6$ singlet

analytically due to the complicated nature of the bare vertex when all E_k terms are included. Solving numerically would also appear to be difficult since there are four orbital indices involved. Progress can be made, though, by defining

$$\bar{\Gamma}^{be} = \Gamma^{b+n, e, b, e+n}; \quad (13)$$

with this definition, Eq. (1) reduces to

$$\tilde{\Gamma}^{be} = \tilde{\Gamma}_0^{be} - \sum_f \tilde{\Gamma}_0^{bf} \chi_0^{f,f} + n \tilde{\Gamma}^{fe}. \quad (14)$$

Thus, an N^4 matrix equation has been reduced to an N^2 matrix equation for each value of n ($n=0$ are the longitudinal bubbles, the rest are transverse bubbles). This is easily solved on the computer given input values for the E_k and χ_0 .

The E_k parameters were taken from Goldschmidt.³⁶ They have been fit to uranium ion data (the level scheme for $\chi_0=0$ in Fig. 5 differs in some quantitative details from the experimental level scheme of Fig. 2 since the spin-orbit interaction has not been included at this point). These parameters are on average 62% of their Hartree-Fock values due to screening. By comparing to the high-energy neutron scattering data of Osborn *et al.* on UPt_3 ,¹⁶ these parameters should be reduced by another 28% when going into the solid. The latter effect is only of quantitative significance and is based on one transition which is seen (assumed to be from 3H_4 to 3F_2), so is ignored in order to use the well-established values of E_k listed in Goldschmidt's article. Hopefully, detailed solid-state values of these parameters will become available with further experimental work. An additional note is that the fitted E_0 is referenced to some arbitrary value of the energy zero, so has no intrinsic meaning. The value listed in the Goldschmidt article, though, gives an F_0 of 1.83 eV, which is fortuitously close to estimates of the screened Coulomb U for uranium,⁴¹ so we retain it without adjustment.

A final comment concerns the energy zero of the problem. Superconductivity involves an instability of the Fermi surface. For a uranium ion, two f electrons are occupied. Even in band-structure calculations for UPt_3 , the number of occupied $j = \frac{5}{2}$ f electrons is just above two. Thus the term E_0 (the Coulomb repulsion between the two f electrons) is already included in the definition of

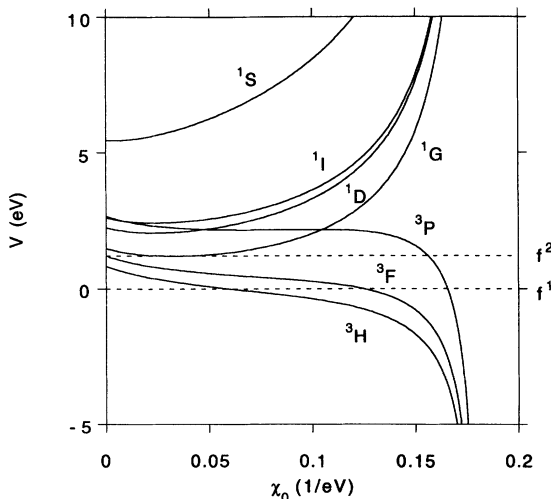


FIG. 5. Effective interaction (LS) in eV for 3H , 3F , 3P , 1I , 1G , 1D , and 1S versus χ_0 for parameters appropriate to a U ion (Refs. 36,41) ($E_0=1225$ meV, $E_1=470.3$ meV, $E_2=1.923$ meV, $E_3=43.28$ meV). The zeros of energy for the f^1 and f^2 cases are marked by the dashed lines.

Fermi energy and represents the zero of energy for the uranium problem (for the cerium case, where only one f electron is occupied, E_0 is not included in the energy zero, since it represents the energy of f^2 above f^1). But the energy term for the $L=5$ ground state of an f^2 ion is $E_0 - 9E_3$. What about the term E_3 ? Since this term cannot be reduced to an effective single-particle form, it would not seem to enter into the definition of the quasiparticle Fermi energy. This gives the rather bizarre result that the $L=5$ vertex is already attractive at the bare interaction level. Of course, one could imagine a scenario where one considered an f^2 - f^3 Anderson lattice model, with the effects of E_3 built into the ground states. The effective quasiparticle operators in this case might implicitly contain the effects of E_3 . Since a detailed theory of this has not been worked out yet, we cannot make any definitive conclusions one way or the other. Since the effective interaction, though, strongly departs from the bare value as χ_0 increases from zero, this question is of minor significance. For purposes of this paper, we assume that the energy zero is at E_0 for the f^2 case and 0 for the f^1 case.

In Fig. 5, Γ is plotted for the triplet states $L=5,3,1$ and for the singlets $L=6,4,2,0$. Just as found for the ${}^3\text{He}$ problem, the triplet interactions are attractive and the singlet ones repulsive, with an instability in both cases at $(E_0 + 9E_1)\chi_0 = 1$. Note that this criterion is a combination of the two analytic results discussed above; thus the instability has both a localization and a magnetic component. This observation indicates that the debate concerning both ${}^3\text{He}$ and heavy fermions about whether the physics is nearly localized or nearly magnetic is merely semantics, as both effects are intertwined. A significant difference from the ${}^3\text{He}$ case is the effect of orbital interactions in the current problem. In ${}^3\text{He}$, the orbital degeneracy of the pair state is lifted by Fermi-surface projection of the vertex; in the f -electron case, this degeneracy is already lifted by the interaction itself. Note that the largest attractive instability is for $L=5, S=1$ (in such a state, the Coulomb repulsion is minimized). Thus, the pair state is predicted to satisfy both Hund's first and second rules, and is a generalization of the results obtained for ${}^3\text{He}$. A similar result has been obtained by van der Marel and Sawatzky based on the Anderson model.³³

We now turn to a discussion of the problem at the JJ -coupling level, which, as argued above, is more physically relevant at the quasiparticle level than the LS scheme (or even the intermediate-coupling scheme). The bare interaction vertex can be gotten by replacing the orbital-spin indices of Eq. (2) by the indices μ which range from $-\frac{5}{2}$ to $\frac{5}{2}$ (we assume only $j = \frac{5}{2}$ quasiparticles are involved). By taking into account the mixed spinor nature of the relativistic orbitals, the formulas for c_k can be calculated in a manner similar to that used on p. 217 of Ref. 31. Note that only $k=2$ and 4 are involved ($k=6$ comes in when considering $j = \frac{7}{2}$ states). The resulting expressions were checked against tabulated results on p. 560 of Ref. 42. As in the LS case, the F_k are not useful in exploiting the group properties of the f electrons, so one rotates to another basis E_k . It should be noted that these

E_k are not the same E_k as in the LS case. They have been discussed in the context of nuclear physics, where JJ coupling has been traditionally of more use,⁴³ and the analogous e_k coefficients are listed in Table III. In this case, there are only three terms, $J=4,2,0$ (corresponding to $L=5,3,1$ in the LS case). As in the LS case, e_0 is 1 for all states. e_1 is 3 for $J=0$, and 0 otherwise, which has analogies to e_1 in the LS case. In particular, $J=0$ appears at the f^0 level and thus has a different quasispin (i.e., seniority) than $J=2,4$. The term e_2 splits the latter two states apart (similar to e_3 in the LS case). In this notation, the ground-state $J=4$ term is $E_0 - 5E_2$. This is lower than the E_0 energy zero just as found for the $L=5$ LS case. By fitting these values for states of definite J , we can infer an interaction vertex analogous to Van Vleck's⁴⁰ of Eq. (8) for the p -electron LS case:

$$w_{12} = E_0 + \frac{q_{12}}{2} E_1 + [-2\mathbf{j}_1 \cdot \mathbf{j}_2 - \frac{5}{2}(1 + q_{12})] E_2, \quad (15)$$

where q_{12} is a seniority operator ($\langle J | q_{12} | J \rangle = 6\delta_{J0}$) and \mathbf{j} is the total angular momentum operator.

Analogous analytic series can also be constructed. In particular, keeping just E_0 gives an expression like Eq. (10) with 13 replaced by 5 since the orbital degeneracy is now 6 instead of 14.

We now solve Eq. (1) exactly as done for the LS case. The interaction parameters are again obtained from Goldschmidt.³⁶ The results are plotted in Fig. 6. An attractive instability is found for $J=4$, a repulsive instability for $J=2,0$. The instability occurs at a value $(E_0 + E_1 + 12E_2)\chi_0 = 1$. This result is important in that it makes a very definite prediction; if a paramagnonlike picture analogous to ${}^3\text{He}$ applies to heavy-fermion superconductors, a pair state of relative $J=4$ should be realized.

How does this change if we replace uranium by cerium? First, the energy zero does not contain E_0 so that the bare interaction is more repulsive. Second, E_0 is about three times larger since U is around 6 eV for cerium ions.⁴⁴ Although this means that the instability occurs for a smaller value of χ_0 , we expect the interaction to be more repulsive since E_0 is larger. This is illustrated in Fig. 7, which is analogous to Fig. 6 except parameters tabulated by Goldschmidt for the cerium ion are used⁴⁵ (with an E_0 of 6.0 eV). As can be seen, the interaction in all channels is repulsive except very close to the instability for $J=4$. On the other hand, in strong-coupling calculations for the paramagnon model in ${}^3\text{He}$, the calculated superfluid transition temperature actually turns off as the instability is approached since the energy scale of the paramagnon (proportional to $1 - I\chi_0$) is going to zero

TABLE III. f^2 energies in the JJ scheme (Ref. 43). Note that the E_k parameters are different from those defined in the LS scheme.

Term	Energy
$J=4$	$E_0 - 5E_2$
$J=2$	$E_0 + 9E_2$
$J=0$	$E_0 + 3E_1$

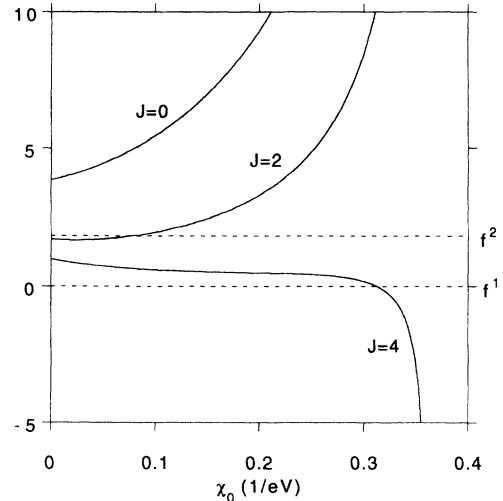


FIG. 6. Effective interaction (JJ) in eV for $J=4,2,0$ versus χ_0 for a U ion. Same parameters and notation as in Fig. 5.

(that is, the T_c maximum is near but not at the instability).⁴⁶ Because of this, pairing is possible for cerium alloys but much less likely than in the uranium case, where one finds a larger range of χ_0 where there is attraction. An alternate view is that a pair wave function with two f quasiparticles has much less overlap with the bare f -ion wave function in the cerium case since the f^2 component in cerium is much smaller than in uranium. This is in accord with experimental observations discussed in the second section.

We now discuss the issue of orbital and momentum dependence of the susceptibility bubble. In heavy-fermion uranium alloys, there is not much evidence for crystal-field effects. This indicates that all the $j = \frac{5}{2}$ orbitals are strongly mixed, as predicted by band theory (as discussed for Kondo lattice models by Zwignagl,⁴⁷ if the Kondo temperature is larger than the crystal-field split-

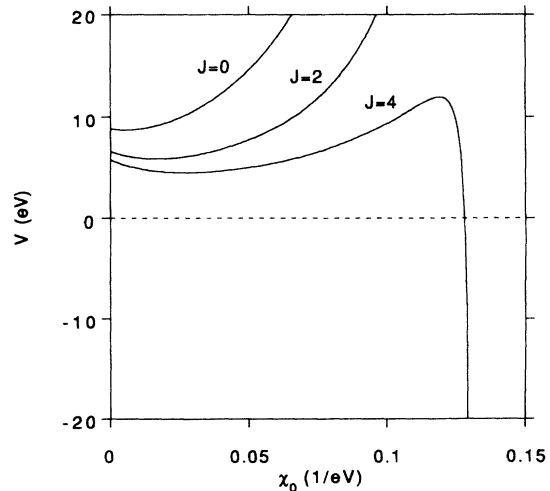


FIG. 7. Effective interaction (JJ) in eV for $J=4,2,0$ versus χ_0 for parameters appropriate to a Ce ion^{45,44} ($E_0=6000$ meV, $E_1=484.5$ meV, $E_2=2.293$ meV, $E_3=47.67$ meV; note these are $LS E_k$). The zero of energy is the dashed line.

tings, then all f -orbital energies get renormalized to the Fermi energy and are intermixed; this appears to be the case in UPt_3). Because of this, one would expect the orbital and momentum dependence of χ_0 to be rather weak. There are intersite interactions, though, which give the full susceptibility, χ , momentum dependence. An argument against the importance of this effect for the pairing has been given by Anderson² where he emphasizes the dominance of the on-site interaction, given the large ratio of T_c to E_F . The issue of intersite pairing will be discussed in the last section. On the other hand, the susceptibility in metals like UPt_3 is strongly dependent on field direction. Whether this is a consequence of crystal-field effects or simply due to intersite correlations is an unresolved matter³ although neutron scattering data in UPt_3 point to the latter.⁶ If this is a crystal-field effect, it can be represented by χ_0 . If χ is maximal for fields along the c axis (as in URu_2Si_2), this indicates that the longitudinal bubbles are dominant. If one redoes Fig. 6 with just longitudinal bubbles, then the J multiplets are split into various M_J terms (actually, those M_J combinations which have the appropriate crystal symmetry) with the maximum M_J configuration having the most attractive instability. On the other hand, if χ is maximal for fields in the basal plane (like in UPt_3) then transverse bubbles with $n=1$ are dominant [n as defined in Eqs. (13) and (14)]. This in turn leads to the minimum M_J configuration being preferred. Higher values of n would indicate the importance of quadrupolar ($n=2$) effects, etc. These terms play an important role in certain theories.^{14,20} These observations are summarized in Table IV (where it should be noted that a $J=4$ state is always preferred). In this paper, these effects will be further ignored, although they are relatively easy to incorporate if they can be accurately determined (and if they are indeed due to χ_0 itself). An argument that these effects cannot be too strong is that an $M_J=0$ pair state is not consistent with experimental data in UPt_3 , since it is a single-dimensional group representation, although similar anisotropic spin-fluctuation work in a spin-only approximation gave an analogous $M_S=0$ pair state,¹⁰ which is consistent with observations of anisotropy in the upper critical field.⁴⁸ These issues will be discussed further in

TABLE IV. Summary of anisotropic Γ for $J=4$ using parameters of Fig. 6. n is the type of bubble used [defined in Eq. (14)], χ_0 is the value (eV^{-1}) at which the divergence occurs, and M signifies which M_J state is the most attractive (with other attractive M_J states listed in parentheses). Note there is no attraction for $n=5$. For $J=2$, attraction is found for $M_J=0$ in the $n=3,4$ cases, but weaker than for $J=4$. For $J=0$, no attraction is found.

n	χ_0	M
0	0.365	4(3)
1	0.365	0(1,2)
2	0.420	0(2)
3	0.420	1
4	0.420	0
5	0.420	—

the next section. As also discussed in the next section, projection of the vertex on the Fermi surface will also lead to lifting of the degeneracy of the J manifold (analogous to the lifting of L degeneracy in ^3He). It is that effect we concentrate on in this paper.

We conclude this section with a discussion of the general vertex. In ^3He , the full vertex can be written in a form analogous to the bare expression in Eq. (3), that is, a density piece proportional to the δ functions and a spin piece proportional to the scalar product of spin operators.²⁷ Given the similarity of Eq. (3) to, say, Eq. (15), this should also be possible in the f -electron case (as long as one restricts oneself to states of definite LS or J). In particular, there will be a density piece, a quasispin (seniority) piece, and an orbital piece proportional to the scalar product of total angular momentum operators. This justifies some of the phenomenological interactions used in previous work.¹³ Further exploitation of these ideas should give us a more fundamental insight into the properties of the full vertex for f electrons. We should note that the screened Slater integrals F_k can be considered as analogues of the Landau F functions of Fermi-liquid theory.

V. APPLICATION TO UPt_3

We now wish to apply the formalism in the previous section to a real heavy-fermion superconductor. We choose for this purpose UPt_3 . There are two good reasons for this. First, a variety of experimental data exist on this metal which gives us a fairly good idea about what the order parameter is. Second, extensive de Haas-van Alphen data⁴⁹ on UPt_3 give a Fermi surface in fairly good agreement with local-density approximation (LDA) band-structure calculations.⁵⁰ This indicates that the momentum dependence of the LDA wave functions is fairly trustworthy. The frequency dependence is not, of course, since the effective mass in the measurements is about 16 times the LDA band mass. This is due to the fact that, in heavy fermions, the self-energy has a large frequency derivative leading to a large mass enhancement. Investigation of transport properties indicates that the momentum derivative of the self-energy must be rather weak so that the self-energy “rides” with the Fermi energy.⁵¹ That is why the shape of the LDA Fermi surface is about correct even though the mass is off by a large factor. These issues are of importance since we want to convert the formalism of the previous section to apply to quasiparticle states. We can do this approximately by taking the four bare external lines of the vertex in Eq. (1) and multiplying each of them by the wave-function renormalization factor $Z^{1/2}$, where as indicated above $1/Z \sim 16$. This represents the effect that only Z of the bare electron is in the quasiparticle pole.

To proceed further, note that for the interaction considered here

$$\langle J, \alpha | \Gamma | J', \alpha' \rangle = \delta_{JJ'} \delta_{\alpha\alpha'} \Gamma_{J, \alpha}, \quad (16)$$

where α is a basis function of J which has the appropriate crystal symmetry. For axial symmetry, this would just be M . For hexagonal symmetry, they are listed in Table V.

TABLE V. Hexagonal basis functions for $J=4$ in terms of M_J . The forms listed in this table should be symmetrized (+ representation) or antisymmetrized (- representation) with respect to the site before use. For Γ_5 , α , and β are variational coefficients such that the sum of their squares is equal to 1, and this representation occurs twice (α, β and $\beta, -\alpha$). Note that Γ_5 and Γ_6 are doublets obtained by replacing $|M_J\rangle$ by $|-M_J\rangle$. These functions in terms of products of single-particle states are given in Ref. 1.

Representation	Basis
Γ_5	$\alpha 4\rangle + \beta -2\rangle$
Γ_3	$\sqrt{\frac{1}{2}}(3\rangle + -3\rangle)$
Γ_4	$\sqrt{\frac{1}{2}}(3\rangle - -3\rangle)$
Γ_6	$ 1\rangle$
Γ_1	$ 0\rangle$

The dependence of Γ on α occurs if anisotropy is put into χ_0 as discussed in the last section. Also, for a multidimensional group representation, Γ will be the same for each α in the representation, unless the symmetry is lowered by some external perturbation. This has relevance for Ginzburg-Landau models of the phase diagram for UPT_3 and will be discussed later. For now, though, we assume only a J dependence for Γ . These are plotted in Fig. 6. Given this, we can now calculate the pairing interaction on the Fermi surface. We do this by constructing the product $|\mathbf{k}, -\mathbf{k}\rangle$ and expanding this in terms of $|J, \alpha\rangle$. The first thing to note is that there are two degenerate states for each $\mathbf{k} \rightarrow (\mathbf{k}, P\mathbf{T}\mathbf{k})$ where P is the parity operator and T the time-reversal one) and two for $-\mathbf{k}$ ($P\mathbf{k}, T\mathbf{k}$).⁵² The combination $\frac{1}{2}(|\mathbf{k}, T\mathbf{k}\rangle - |P\mathbf{T}\mathbf{k}, P\mathbf{k}\rangle)$ defines a pseudospin singlet d_0 . The three combinations

$$\frac{1}{2}(|P\mathbf{T}\mathbf{k}, T\mathbf{k}\rangle - |\mathbf{k}, P\mathbf{k}\rangle) = d_x,$$

$$-\frac{i}{2}(|P\mathbf{T}\mathbf{k}, T\mathbf{k}\rangle + |\mathbf{k}, P\mathbf{k}\rangle) = d_y,$$

and

$$\frac{1}{2}(|\mathbf{k}, T\mathbf{k}\rangle + |P\mathbf{T}\mathbf{k}, P\mathbf{k}\rangle) = d_z$$

define a pseudospin triplet, known as the d vector. In the current approximation, only the part of $|\mathbf{k}, -\mathbf{k}\rangle$ on the same site is involved in Eq. (16). (Note that although the pair interaction is only attractive for particles on the same site, the pairs are correlated out to a distance of the coherence length, much like the problem of bound states of a potential well where the particles spend most of their time outside the well.²⁹) Now, the part of $|\mathbf{k}\rangle$ involving $j = \frac{5}{2}$ states is⁵³

$$|\mathbf{k}\rangle = \sum_{\mu i} a_{\mu i}^{n\mathbf{k}} |\mu\rangle_i, \quad (17)$$

where μ runs from $-\frac{5}{2}$ to $\frac{5}{2}$, i is the f -atom site index (1,2 for UPT_3), and n is the band index (five bands are predicted to cross the Fermi energy in UPT_3). Thus the coefficient of $|\mathbf{k}, -\mathbf{k}\rangle$ involving $j = \frac{5}{2}$ states on the same site with the correct group-representation structure for a

particular total J ($J=0, 2, 4$) is

$$A_{\mathbf{k}}^{J\alpha j} = \hat{P}_{J\alpha j} \sum_{\mu vi} a_{\mu i}^{n\mathbf{k}} a_{vi}^{n-\mathbf{k}}, \quad (18)$$

where j represents the pseudospin combination (0 for singlet, x, y, z for triplet) and \hat{P} is a projection operator which takes that part of the sum which has the form of one of the basis functions with the appropriate pseudospin combination discussed above. Because of antisymmetry, A changes sign from one site to the other site in the unit cell for pseudospin triplets, and does not for pseudospin singlets (for one f atom per cell, only pseudospin singlets exist⁵⁴). Summarizing, the particle-particle vertex is

$$\langle \mathbf{k}', -\mathbf{k}' | \Gamma | \mathbf{k}, -\mathbf{k} \rangle = Z^2 \sum_{J\alpha j j'} \Gamma_J A_{\mathbf{k}'}^{*J\alpha j'} A_{\mathbf{k}}^{J\alpha j}. \quad (19)$$

Since Eq. (19) is separable in \mathbf{k} and \mathbf{k}' , this allows us to write down the BCS coupling constant

$$\lambda_{J\alpha} = N \Gamma_J Z^2 \sum_j \langle |A_{\mathbf{k}}^{J\alpha j}|^2 \rangle_{\mathbf{k}}, \quad (20)$$

where N is the density of states, $\langle \dots \rangle_{\mathbf{k}}$ is an average over a narrow energy shell about the Fermi energy, and j runs over 0 for even parity, x, y, z for odd parity. For UPT_3 , this average was done on a regular grid of 561 \mathbf{k} points in the irreducible wedge ($\frac{1}{24}$) of the Brillouin zone, keeping those $n\mathbf{k}$ states within 1 mRy of the Fermi energy (182 states total). Those points that are in symmetry planes of the zone are plotted in Fig. 8. The number 1 mRy was chosen so as to have enough points to give a good representation of the Fermi surface with this size grid. Note that in this model

$$\Delta_{J\alpha j}(\mathbf{k}) \propto A_{\mathbf{k}}^{J\alpha j}, \quad (21)$$

where Δ is the order parameter.

In Table VI, coupling constants⁵⁵ for UPT_3 are shown

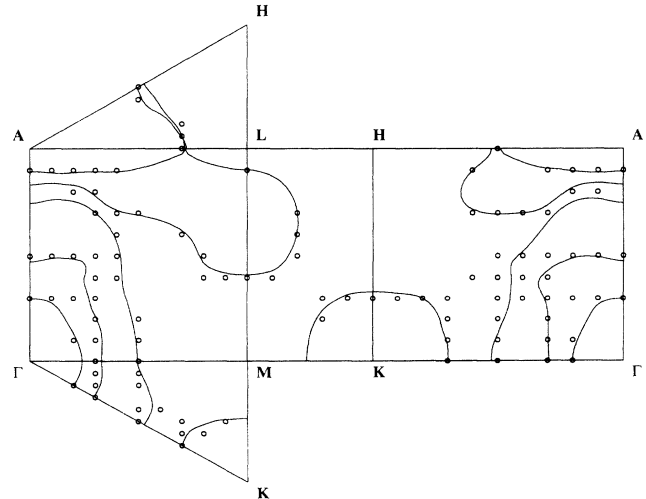


FIG. 8. Plot of the \mathbf{k} points used in the calculations on UPT_3 in symmetry planes of the Brillouin zone constructed from a uniform grid within an energy cutoff of 1 mRy of the Fermi energy. Lines represent the Fermi surface.

TABLE VI. Coupling constants for UPt_3 . These should be multiplied by the quantity $N\Gamma_4 Z^2$ to convert to real coupling constants.

Representation	$J=4(+)$	$J=4(-)$	$J=2(+)$	$J=2(-)$	$J=0(+)$	$J=0(-)$
Γ_5	0.069	0.073				
Γ_5	0.029	0.101	0.049	0.071		
Γ_3	0.024	0.064				
Γ_4	0.013	0.120				
Γ_6	0.018	0.125	0.035	0.106		
Γ_1	0.076	0.114	0.065	0.099	0.495	0.057

modulo $N\Gamma_j Z^2$ with the largest occurring for $J=0, \Gamma_1^+$. This is just the nodeless Balian-Werthamer (BW) state with spin-orbit coupling,⁵⁶ with a coupling constant proportional to the square of the ratio of the $j = \frac{5}{2} f$ density of states to the total density of states. From Fig. 6, though, the $\lambda_{2\alpha}$ and $\lambda_{0\alpha}$ coupling constants are repulsive and so do not play a role. For the attractive $J=4$ case, the largest coupling constants are for odd-parity states. This is because three pseudospin triplet terms contribute to Eq. (20) in this case as opposed to one pseudospin singlet for even-parity states. The importance of this is that pseudospin triplets only exist because of the two f atoms per unit cell, which, as illustrated in Table I, all heavy-fermion superconductors have. This is a property of an on-site pairing theory, and has no relevance in near-neighbor pairing models. The largest coupling constant occurs for $\Gamma_6^- (E_{2u})$ symmetry, although several other states have comparable sized coupling constants (Γ_1^-, Γ_4^-). Note that this is an odd-parity two-dimensional group representation.

Let us discuss this state. For the odd-parity case, the order parameter is a vector. At a general \mathbf{k} , all three components are involved because of the relativistic nature of the wave-function coefficients. For two-dimensional group representations, this means that the state will be nonunitary ($\mathbf{d} \times \mathbf{d}^* \neq 0$). A discussion of the case of nonunitary d vectors can be found in Ref. 57; they play a major role in a recent phenomenological theory of UPt_3 .⁵⁸ In the nonunitary case, there are two gaps for each \mathbf{k} ,

$$\Delta_\sigma(\mathbf{k})^2 = |\mathbf{d}(\mathbf{k})|^2 + \sigma |\mathbf{d}(\mathbf{k}) \times \mathbf{d}^*(\mathbf{k})|^2, \quad (22)$$

where σ is \pm . Plots of this for the Γ_6^- state are shown in Figs. 9 and 10 with the total density of states shown in Fig. 11. No attempt has been made to fit these gaps to simple functions⁵⁹ because the complex momentum dependence of the wave functions would prohibit this. Instead, some general properties can be inferred. For instance, the d_z component vanishes for $k_z=0$ as expected from earlier work.⁶⁰ A surprise, though, is that all three d vector components vanish on the zone face $k_z = \pi/c$. Thus, this state has a line node gap function, and provides a counter argument to earlier statements that line node gap functions are not possible for odd-parity states.⁶⁰ Moreover, all d vector components vanish along the axis $k_x=0, k_y=0$ which gives rise to point nodes. A gap function of this sort (line nodes perpendicular to the c axis, point nodes along the c axis) is consistent with a

variety of experimental data in UPt_3 , including specific heat,⁶¹ transverse ultrasound,⁶² penetration depth,⁶³ thermal conductivity,⁶⁴ NMR,⁶⁵ and tunneling⁶⁶ data. Note that, despite the small value of the second gap in Fig. 10, no ‘‘normal’’ component is seen in the density of states of Fig. 11. Thus, this nonunitary state differs from the one considered by Machida and co-workers⁵⁸ where one of the gap components vanishes identically for all \mathbf{k} so that there is a normal component with half the value of the normal state (in the theory of Coleman, Miranda, and Tsvelik,¹⁵ a similar normal component occurs). It should be remarked that, although earlier specific heat data⁶¹ indicated a sizable normal component, this is probably due to impurity effects since newer data do not show this component.⁶⁷ As for the two-dimensional nature of the group representation, our current understanding of the field-temperature-pressure phase diagram of UPt_3 is in strong support of such a state.^{12,68,69} In particular, weak magnetism is present which lowers the symmetry to orthorhombic. This acts to split the superconducting transition into two transitions. Pressure acts to eliminate both the magnetism and the splitting,⁷⁰ thus giving strong support for a two-dimensional group representation, as opposed to two nearly degenerate single-dimensional group representations. The main problem with this scenario is the presence of a term in the gradient part of the free energy which tends to mix the two components

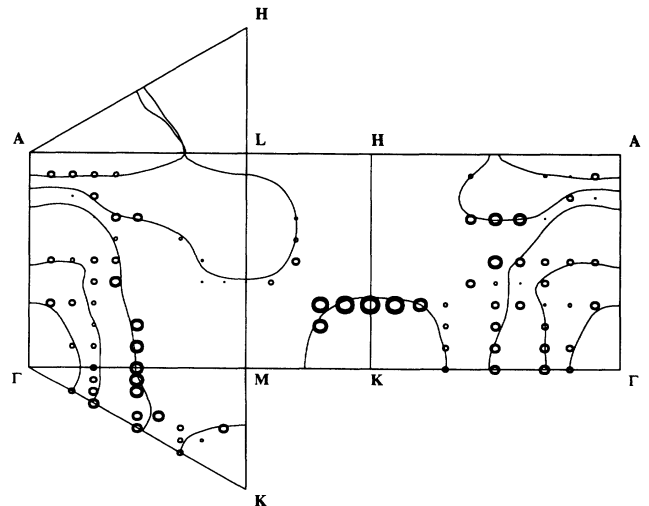


FIG. 9. Plots of $|\Delta_\sigma(\mathbf{k})|$ with $\sigma = +$ for Γ_6^- state on the grid of points of Fig. 8. Size of the dots represents the magnitude of the gap. Where no dots appear, the gap is zero or very small.

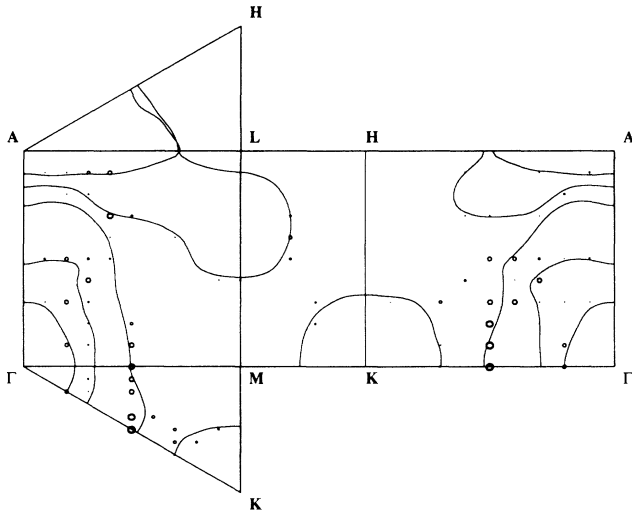


FIG. 10. Same as Fig. 9, but with $\sigma = -$.

of the representation except for certain field directions. This is in contradiction to experiment, which shows a fairly isotropic phase diagram with respect to field direction (this was the main motivation for the nearly degenerate model^{71,72}). Sauls, though, has shown that for an axially symmetric Fermi surface and axially symmetric basis functions, this mixing term is zero for the E_2 representation.¹² In the general case, it is not, but its mixing term is smaller than that of the E_1 representation. This work will be discussed in another paper,⁷³ but it suffices to say here that, for the current theory, the mixing term for our $\Gamma_6^-(E_{2u})$ state is small enough so as to be promising in regards to explaining the phase diagram. Alternate theories based on two nearly degenerate representations^{71,72,74} are also consistent with the current theory, given the closeness of the coupling constants for Γ_6^- , Γ_1^- , and Γ_4^- (the last state having the same line node structure as Γ_6^-).

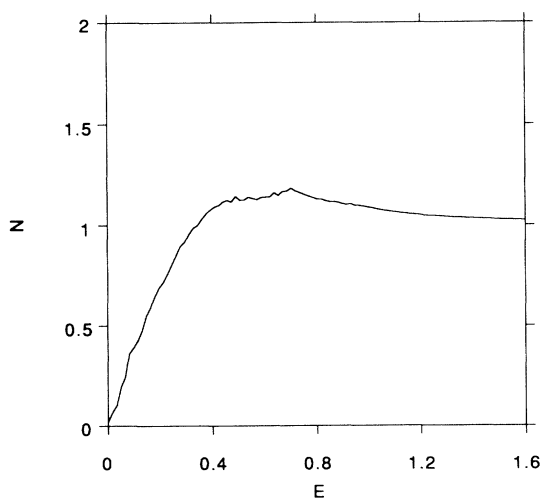


FIG. 11. Smoothed fit to the density of states (normalized to the normal-state value) constructed from the gaps plotted in Figs. 9 and 10. Energy units are normalized to the value of the largest gap.

A final issue concerns the question of parity. No change below T_c for UPt_3 has been seen in the Knight shift⁷⁵ or induced-moment form factor,⁷⁶ indicating no change in the magnetic susceptibility below T_c . This is in support of an odd-parity state, although one could argue that, in the heavy fermions, the quasiparticle (intra-band) part of the susceptibility is small compared to the Van Vleck (inter-band) part, so this conclusion is not definitive. Choi and Sauls⁴⁸ have also shown that the observed low-temperature directional anisotropy of the upper critical field⁷⁷ is most easily explained with an odd-parity pair state with $M_S = 0$ (note, the quantization axis is assumed to be along c). Such a state came out of earlier nonrelativistic spin-fluctuation calculations which took into account the directional anisotropy of the susceptibility.¹⁰ In the current case, though, spin and orbital components are mixed and so a pure $M_S = 0$ state is not possible. On the other hand, the state found here, $|M_J| = 1$, has the largest projection of J on the basal plane of any two-dimensional group representation ($M_J = 0$ has the largest projection, but is one dimensional), so is promising in that regard. To test this quantitatively would require a detailed calculation of the upper critical field with both spin and orbital degrees of freedom taken into account. Certainly, if the current predicted state is correct, the H_{c2} anisotropy cannot just be a spin effect as envisioned by Choi and Sauls. This can be seen as follows. A direct translation of their idea to the current state would be to have a state of pure d_z character in pseudospin space. This can be tested by rotating in pseudospin space at each \mathbf{k} so that the state $|\mathbf{k}\rangle$ has maximal J_z along the chosen quantization axis. This was done for quantization axes along the a , b , and c axes of the hexagonal crystal (for the a and b case, this lowers the system to orthorhombic symmetry). In all cases, the averages $\langle |d_i|^2 \rangle_{\mathbf{k}}$ were within 20–30% of each other, i.e., there is no dominant d_z component. This is consistent with the highly nonunitary nature of this state seen in Figs. 9 and 10. As indicated above, then, orbital effects in the upper critical field must be playing an important role. This would require a theory for calculating H_{c2} for a nonunitary multicomponent d vector in the strong spin-orbit coupling limit.

We finally turn to a discussion of T_c . We should note that the density of states already contains the renormalization factor $1/Z$ (i.e., $N = N_0/Z$ where N_0 is the bare density of states). This means that the prefactor $N\Gamma_J Z^2$ in Eq. (20) is analogous to the form $\lambda_\Delta/(1 + \lambda_Z)$ found in strong-coupling theories,⁴⁶ since $N_0\Gamma_J$ would be the pairing coupling constant λ_Δ , and $1/Z - 1$ would be the mass coupling constant λ_Z . This is consistent with the fact that renormalization of the external lines of the vertex is a strong-coupling effect. On the other hand, the frequency dependence of the bubble has not been kept, so one has to simulate this by providing an energy cutoff of order of the renormalized Fermi energy. We note that the size of the specific heat coefficient³ and the neutron scattering linewidth⁶ are consistent with a renormalized energy scale for UPt_3 of order 5 meV. This is also consistent with estimating a band-structure Fermi energy and multiplying this by Z . The last thing to be deter-

mined is Γ_J . This is made difficult by the fact that χ_0 is being treated as a number in this paper, whereas in reality it is a highly complicated function of momentum, frequency, and band and orbital indices. Given the strong dependence of Γ_J on χ_0 (and also the question of the energy zero), the exponential dependence of T_c on coupling constant, and the uncertainties mentioned in the above approximations, the most illustrative approach is just to see what value of χ_0 is needed to obtain the observed T_c . With a T_c of 0.5 K and a cutoff of 5 meV, this gives a value for λ of 0.205. Since $\lambda = N\Gamma_4 Z^2 c$ where c from Table VI for $J=4$, Γ_6^- is 0.125, this gives a Γ_4 of -2.1 eV relative to the energy zero. From Fig. 6, this gives a χ_0 of 0.335, which is 0.92 of the divergence value, giving a Stoner renormalization of 12, comparable to the mass renormalization value of 16 assumed from the beginning. Since spin-fluctuation models based on the observed heavy-fermion dynamic susceptibility have a mass renormalization which goes like the Stoner factor, as opposed to the logarithm of the Stoner factor which one gets for a Lindhard function,⁸ then there is overall consistency in these numbers. This can be further demonstrated by estimating χ , obtained by multiplying χ_0 by the Stoner renormalization (12) then by the square of the orbital degeneracy (36). This gives a value of about 150 states/eV, comparable to the 180 states/eV given by the specific heat γ of 420 mJ/mol K².³ Moreover, converting χ to proper units (with $g = \frac{6}{7}$ and $j = \frac{5}{2}$) gives 0.0075 emu/mol, comparable to data from susceptibility measurements.³ To obtain a more reliable estimate of these parameters would require doing a full strong-coupling calculation retaining the frequency dependence of the bubble.⁴⁶

The large estimated size of Γ_J of order 2 eV which must be renormalized downwards by Z^2 might seem somewhat worrisome. After all, wouldn't one expect high T_c in transition metals where Z is closer to 1? The question of renormalizing the interaction downwards has been discussed by Anderson² and reviewed by Lee *et al.*⁷⁸ The main point to emphasize here is that the interaction parameters of this paper are only appropriate for a system close to an f^2 configuration, and the same thing that is causing the large value of Γ_J is also causing a small value for Z . In transition metals, the E_k parameters are largely screened out and play no role. Instead, one collapses back to standard spin-fluctuation model with a Stoner interaction parameter I . Estimates based on this I give extremely low estimates of T_c , even in palladium which has a large Stoner renormalization.⁷⁹

VI. FUTURE DIRECTIONS

An advantage of the current approach is that the theory is systematically improvable by removing various approximations made in this paper. The most severe of these is treating χ_0 as a number. A proper strong-coupling calculation would include the frequency dependence of this object. This is not too difficult if the simple relaxational form is used,

$$\chi_0(\omega) = \frac{\chi_0 \Gamma}{\Gamma - i\omega}, \quad (23)$$

where Γ is the neutron scattering linewidth.⁶ Work of this sort has been done in earlier spin-fluctuation models.^{8,10} Of more interest is the momentum and orbital dependence of this object. The philosophy of this paper is similar to that espoused early on by Anderson,² that is the size of the effective interaction is large enough (large ratio of T_c to E_F) that the on-site interaction must play the central role. This is also consistent with the observation that one of the defining properties of the heavy-fermion metals is their large f -atom separation,⁸⁰ giving weak intersite interaction effects. Even neutron scattering data indicate that part of the susceptibility where the bulk of the fluctuating moment is has a relatively mild momentum dependence.⁶ On the other hand, these effects played a crucial role in earlier spin-fluctuation models, so it is of interest to see how they would enter the current formalism. In the real-space approach taken here, these effects would be simulated by adding a term $\chi_0(R, R')$ in addition to the term $\chi_0(R, R)$ where R, R' are site indices with R' a near neighbor of R . Near-neighbor effects would show up in Eq. (1) at first order in this bubble. At second order in this bubble, there would be terms which would also affect on-site pairing [$\chi_0(R, R')\chi_0(R', R)$]. Assuming Eq. (1) can be solved, one is left with a vertex which contains on-site terms, near-neighbor terms, etc. The general properties of this vertex along with the functional forms of the near-neighbor and next-near-neighbor pairs are discussed by Appel and Hertel.⁵

We illustrate these ideas in the following manner. Let us assume the following form for χ_0 :⁹

$$\chi_0(\mathbf{q}) = \chi_0 + \chi_1 \sum_{R'} e^{i\mathbf{q}\cdot(\mathbf{R}' - \mathbf{R})}, \quad (24)$$

where R' is a next near neighbor of R . We consider the next-near-neighbor case for this part of the argument since multiband effects do not have to be explicitly invoked (for the UPt₃ lattice, next near neighbors are separated by a primitive lattice vector, but near neighbors are separated by a nonprimitive lattice vector, so multiband effects have to be considered in that case). A positive χ_1 corresponds to the ferromagnetic case and a negative one to the antiferromagnetic case. We now solve Eq. (14) for each \mathbf{q} , giving $\Gamma(\mathbf{q})$. We then determine $\Gamma(R, R', R, R')$ by Fourier transforming $\Gamma(\mathbf{q})$. Note that since the two electrons are not at the same site, odd- J states are now allowed. What is found is that for the ferromagnetic case, the largest attraction occurs for maximal J ($J=5$), whereas for the antiferromagnetic case, the largest attraction occurs for minimal J ($J=0$). This is analogous to the single-orbital result of $S=1$ and 0, respectively, which was discussed at the end of Sec. III. As expected, the size of this interaction can be comparable to the on-site component if the q dependence is strong enough.

For the antiferromagnetic case, we construct pair states of relative $J=0$ for both near-neighbor and next-near-neighbor cases as derived by Appel and Hertel.⁵ For near-neighbor pairs with $J=0$, only the representations Γ_1^+ , Γ_3^+ , Γ_5^+ , and Γ_6^+ occur. For next-near-

neighbor pairs, only Γ_1^+ , Γ_1^- , Γ_5^+ , and Γ_5^- occur. These multiple representations occur due to summation over the six neighbors in each case. In Table VII, the resulting coupling constants are shown. In both cases, the Γ_1^+ coupling constant is by far the largest, similar to earlier work based on phenomenological interactions.¹³ Unlike the on-site case, these Γ_1^+ states have nodes, but, as they are single-component order parameters, they cannot explain the experimental data in UPt_3 . This is another strong argument against the relevance of near-neighbor pairing for heavy-fermion superconductors.

The other issue concerns orbital dependence of the bubble. Calculations of this sort exist in the literature for UPt_3 ,⁸¹ and are rather tedious, as they involve calculating matrix elements of relativistic wave functions over a fine enough grid in \mathbf{k} space to get reliable values of χ_0 . As discussed in Sec. IV, one might get around this difficulty by simulating these effects with some effective crystal-field model. The most probable picture based on the temperature dependence of the neutron scattering data, though, is that this effect enters most prominently in the $\chi_0(R, R')$ term.⁶

The next issue concerns feedback effects which are important in the physics of superfluid ^3He . In that case, all $L=1$ states are degenerate at T_c . Therefore, one would expect the isotropic state, the BW state, to have the lowest free energy. On the other hand, the susceptibility changes below T_c which affects the pair interaction and favors states with maximal anisotropy, giving rise to the Anderson-Brinkman-Morel (ABM) state.^{27,29} In the current problem, though, (1) this degeneracy is already broken in the normal state due to the crystal lattice and (2) there is no experimental evidence for a change in the susceptibility below T_c (based on Knight shift⁷⁵ and induced-moment form factor⁷⁶ measurements), although it should be noted that the interband, or Van Vleck, component most likely dominates the susceptibility.⁸¹ (Neutron scattering experiments which access the low-momentum, low-frequency part of the dynamic susceptibility would be helpful in extracting out the quasiparticle part of the susceptibility and seeing how it changes below T_c .) Because of this, feedback effects probably do not play an important role in the heavy-fermion problem (the large ratio of T_c to E_F would argue against this, though). A related effect is whether the interaction changes as a function of field (this could be connected to the H_{c2} anisotropy discussed in the previous section). Magnetization data look very linear in field for all field directions for the field range of interest³ which would argue against this. On the other hand, as T_c depends exponentially on coupling constant, small changes in the quasiparticle wave functions in an applied field could lead to noticeable effects, especially given the low effective Fermi energy. This could be simulated in the current theory by rediagonalizing the band-structure wave functions in the presence of the appropriate field and seeing how the coupling constants listed in Table VI change.

TABLE VII. Coupling constants for UPt_3 for the case of near-neighbor (NN) and next-near-neighbor (NNN) pairing with $J=0$. These should be multiplied by the quantity $N\Gamma_0 Z^2$ to convert to real coupling constants with Γ_0 referring to the $J=0$ NN or NNN component of the Fourier transform of $\Gamma(\mathbf{q})$.

NN	$J=0$	NNN	$J=0$
Γ_1^+	0.134	Γ_1^+	0.351
Γ_3^+	0.075	Γ_1^-	0.044
Γ_5^+	0.079	Γ_5^+	0.178
Γ_6^+	0.066	Γ_5^-	0.020

A related effect is the observed splitting of T_c in UPt_3 that was discussed in the previous section. This has been treated in the past by a phenomenological symmetry-breaking field thought to be due to the orthorhombic distortion associated with the weak antiferromagnetism.⁸² This could also be simulated in the current model by applying a weak staggered field (the new orthorhombic cell would contain four uranium atoms) and rediagonalizing the band-structure wave functions, from which the splitting of the coupling constants could be determined.

The author would like to conclude by saying that the physics of heavy-fermion superconductors is complicated enough (as this paper demonstrates) that the picture offered here may not be complete. On the other hand, he feels that the ultimate theory for these materials must look in some form like what is being proposed here, since the orbital dependence of the f electrons and the short-range nature of the interactions should play a crucial role. It is promising that this model has certain qualitative features reflected in the data (preference for uranium, importance of two f atoms per unit cell) which are hard to understand from earlier spin-fluctuation theories. Also, the predicted pair state for UPt_3 has many promising aspects also missing in earlier theories. Moreover, there is a conceptual beauty to having a pair state which has maximal L and maximal S , as this is a direct generalization of the physics of ^3He with which heavy fermions share many qualitative features. Hopefully, with increased experimental and theoretical effort, we can determine whether this is indeed the right approach to pursue for solving this problem.

ACKNOWLEDGMENTS

This work was supported by U.S. Department of Energy, Office of Basic Energy Sciences, under Contract No. W-31-109-ENG-38. The author would like to acknowledge the hospitality of the Physics Department, Uppsala University, where this work was begun, and to thank Seb Doniach, Kathryn Levin, and Jim Sauls for helpful discussions. The author is indebted to Professor van der Marel for bringing his work with Sawatzky to the author's attention.

- ¹M. R. Norman, *Phys. Rev. Lett.* **72**, 2077 (1994).
- ²P. W. Anderson, *Phys. Rev. B* **30**, 1549 (1984).
- ³A. deVisser, A. Menovsky, and J. J. M. Franse, *Physica B* **147**, 81 (1987).
- ⁴P. W. Anderson, *Phys. Rev. B* **32**, 499 (1985).
- ⁵J. Appel and P. Hertel, *Phys. Rev. B* **35**, 155 (1987).
- ⁶G. Aeppli *et al.*, *Phys. Rev. Lett.* **58**, 808 (1987); A. I. Goldman *et al.*, *Phys. Rev. B* **36**, 8523 (1987); P. Frings *et al.*, *Physica B* **151**, 499 (1988); G. Aeppli *et al.*, *Phys. Rev. Lett.* **60**, 615 (1988); **63**, 676 (1989).
- ⁷K. Miyake, S. Schmitt-Rink, and C. M. Varma, *Phys. Rev. B* **34**, 6554 (1986); D. J. Scalapino, E. Loh, Jr., and J. E. Hirsch, *Phys. Rev. B* **34**, 8190 (1986); M. T. Beal-Monod, C. Bourbonnais, and V. J. Emery, *ibid.* **34**, 7716 (1986).
- ⁸M. R. Norman, *Phys. Rev. Lett.* **59**, 232 (1987).
- ⁹W. Putikka and R. Joynt, *Phys. Rev. B* **37**, 2372 (1988); *ibid.* **39**, 701 (1989).
- ¹⁰M. R. Norman, *Phys. Rev. B* **43**, 6121 (1991); **41**, 170 (1990); **39**, 7305 (1989); **37**, 4987 (1988).
- ¹¹M. R. Norman, *Physica C* **194**, 203 (1992).
- ¹²J. A. Sauls, *J. Low Temp. Phys.* **95**, 153 (1994).
- ¹³M. R. Norman, *Phys. Rev. B* **48**, 6315 (1993).
- ¹⁴D. L. Cox (unpublished).
- ¹⁵P. Coleman, E. Miranda, and A. Tselik, *Phys. Rev. Lett.* **70**, 2960 (1993).
- ¹⁶R. Osborn, K. A. McEwen, E. A. Goremychkin, and A. D. Taylor, *Physica B* **163**, 37 (1990).
- ¹⁷A. Grauel *et al.*, *J. Appl. Phys.* **73**, 5421 (1993).
- ¹⁸K. Andres, S. Darack, and H. R. Ott, *Phys. Rev. B* **19**, 5475 (1979).
- ¹⁹G. J. Nieuwenhuys, *Phys. Rev. B* **35**, 5260 (1987).
- ²⁰D. L. Cox, *Phys. Rev. Lett.* **59**, 1240 (1987).
- ²¹W. J. L. Buyers and T. M. Holden, in *Handbook on the Physics and Chemistry of the Actinides*, edited by A. J. Freeman and G. H. Lander (North Holland, Amsterdam, 1985), Vol. 2, p. 239.
- ²²J.-S. Kang *et al.*, *Phys. Rev. B* **41**, 6610 (1990); D. L. Cox (private communication).
- ²³D. E. Beck, *Mol. Phys.* **14**, 311 (1968).
- ²⁴K. A. Brueckner, T. Soda, P. W. Anderson, and P. Morel, *Phys. Rev.* **118**, 1442 (1960); V. J. Emery and A. M. Sessler, *Phys. Rev.* **119**, 43 (1960).
- ²⁵N. F. Berk and J. R. Schrieffer, *Phys. Rev. Lett.* **17**, 433 (1966).
- ²⁶A. Layzer and D. Fay, *Int. J. Magn.* **1**, 135 (1971).
- ²⁷P. W. Anderson and W. F. Brinkman, *Phys. Rev. Lett.* **30**, 1108 (1973); in *The Physics of Liquid and Solid Helium, Part II*, edited by K. H. Bennemann and J. B. Ketterson (Wiley, New York, 1978), p. 177.
- ²⁸S. Nakajima, *Prog. Theor. Phys.* **50**, 1101 (1973).
- ²⁹A. J. Leggett, *Rev. Mod. Phys.* **47**, 331 (1975).
- ³⁰K. Levin and O. T. Valls, *Phys. Rep.* **98**, 1 (1983).
- ³¹E. U. Condon and H. Odabasi, *Atomic Structure* (Cambridge University, Cambridge, England, 1980).
- ³²S. Doniach, *Phys. Rev. Lett.* **18**, 554 (1967); J. R. Schrieffer, *ibid.* **19**, 644 (1967).
- ³³D. van der Marel and G. A. Sawatzky, *Solid State Commun.* **55**, 937 (1985).
- ³⁴K. Levin and O. T. Valls, *Phys. Rev. B* **20**, 105 (1979); **20**, 120 (1979).
- ³⁵R. J. Radtke, S. Ullah, K. Levin, and M. R. Norman, *Phys. Rev. B* **46**, 11975 (1992).
- ³⁶Z. B. Goldschmidt, *Phys. Rev. A* **27**, 740 (1983).
- ³⁷R. C. Albers, A. M. Boring, and N. E. Christensen, *Phys. Rev. B* **33**, 8116 (1986).
- ³⁸G. Racah, *Phys. Rev.* **76**, 1352 (1949).
- ³⁹B. R. Judd, *Operator Techniques in Atomic Spectroscopy* (McGraw-Hill, New York, 1963).
- ⁴⁰J. H. Van Vleck, *Phys. Rev.* **45**, 412 (1934).
- ⁴¹J. F. Herbst and R. E. Watson, *Phys. Rev. Lett.* **34**, 1395 (1975).
- ⁴²A. de-Shalit and I. Talmi, *Nuclear Shell Theory* (Academic, New York, 1963).
- ⁴³B. H. Flowers, *Proc. R. Soc. London Ser. A* **212**, 248 (1952); A. R. Edmonds and B. H. Flowers, *ibid.* **214**, 515 (1952).
- ⁴⁴A. J. Freeman, B. I. Min, and M. R. Norman, in *Handbook on the Physics and Chemistry of Rare Earths*, edited by K. A. Gschneidner, Jr., L. Eyring, and S. Hufner (North-Holland, Amsterdam, 1987), Vol. 10, p. 165.
- ⁴⁵Z. P. Goldschmidt, in *Handbook on the Physics and Chemistry of Rare Earths*, edited by K. A. Gschneidner, Jr., and L. Eyring (North-Holland, Amsterdam, 1978), Vol. 1, p. 1.
- ⁴⁶K. Levin and O. T. Valls, *Phys. Rev. B* **17**, 191 (1978).
- ⁴⁷G. Zwirnagl, *J. Magn. Magn. Mater.* **76-77**, 16 (1988).
- ⁴⁸C. H. Choi and J. A. Sauls, *Phys. Rev. Lett.* **66**, 484 (1991); *Phys. Rev. B* **48**, 13 684 (1993).
- ⁴⁹L. Taillefer and G. G. Lonzarich, *Phys. Rev. Lett.* **60**, 1570 (1988).
- ⁵⁰M. R. Norman, R. C. Albers, A. M. Boring, and N. E. Christensen, *Solid State Commun.* **68**, 245 (1988).
- ⁵¹C. M. Varma, *Phys. Rev. Lett.* **55**, 2723 (1985).
- ⁵²P. W. Anderson, *Phys. Rev. B* **30**, 4000 (1984); K. Ueda and T. M. Rice, *ibid.* **31**, 7114 (1985).
- ⁵³In the linear muffin-tin orbital formalism employed here, there are radial functions and their energy derivatives involved in the variational wave functions. The latter terms are small in the current case and can be ignored in the coupling-constant calculations.
- ⁵⁴The relativistic $J=4$ pair state is primarily $L=5$, $S=1$ in nature, but this has no relation to the pseudospin character of the pair state.
- ⁵⁵ Γ_5 from Table V involves two coefficients (α and β) which can be determined by a simple variational method applied to Eq. (20). Note they are real numbers.
- ⁵⁶R. Balian and N. R. Werthamer, *Phys. Rev.* **131**, 1553 (1963).
- ⁵⁷M. Sigrist and K. Ueda, *Rev. Mod. Phys.* **63**, 239 (1991).
- ⁵⁸T. Ohmi and K. Machida, *Phys. Rev. Lett.* **71**, 625 (1993); K. Machida, T. Ohmi, and M. Ozaki, *J. Phys. Soc. Jpn.* **62**, 3216 (1993).
- ⁵⁹S. Yip and A. Garg, *Phys. Rev. B* **48**, 3304 (1993).
- ⁶⁰G. E. Volovik and L. P. Gor'kov, *Zh. Eksp. Teor. Fiz.* **88**, 1412 (1985) [*Sov. Phys. JETP* **61**, 843 (1985)]; E. I. Blount, *Phys. Rev. B* **32**, 2935 (1985).
- ⁶¹R. A. Fisher *et al.*, *Phys. Rev. Lett.* **62**, 1411 (1989); K. Hasselbach, L. Taillefer, and J. Flouquet, *ibid.* **63**, 93 (1989).
- ⁶²B. S. Shivaram, Y. H. Jeong, T. F. Rosenbaum, and D. G. Hinks, *Phys. Rev. Lett.* **56**, 1078 (1986).
- ⁶³C. Broholm *et al.*, *Phys. Rev. Lett.* **65**, 2062 (1990).
- ⁶⁴K. Behnia *et al.*, *J. Low Temp. Phys.* **84**, 261 (1991).
- ⁶⁵Y. Kohori *et al.*, *J. Phys. Soc. Jpn.* **57**, 395 (1988).
- ⁶⁶G. Goll, H. v. Lohneysen, I. K. Yanson, and L. Taillefer, *Phys. Rev. Lett.* **70**, 2008 (1993).
- ⁶⁷J. P. Brison *et al.*, *J. Low Temp. Phys.* **95**, 145 (1994).
- ⁶⁸R. Joynt, *J. Magn. Magn. Mater.* **108**, 31 (1992).
- ⁶⁹R. Joynt, *Phys. Rev. Lett.* **71**, 3015 (1993).
- ⁷⁰S. M. Hayden, L. Taillefer, C. Vettier, and J. Flouquet, *Phys. Rev. B* **46**, 8675 (1992).
- ⁷¹R. Joynt, V. P. Mineev, G. E. Volovik, and M. E. Zhitomir-

- sky, *Phys. Rev. B* **42**, 2014 (1990).
- ⁷²D.-C. Chen and A. Garg, *Phys. Rev. Lett.* **70**, 1689 (1993); A. Garg and D.-C. Chen, *Phys. Rev. B* **49**, 479 (1994).
- ⁷³V. Vinokur, J. A. Sauls, and M. R. Norman (unpublished).
- ⁷⁴M. E. Zhitomirski and I. A. Luk'yanchuk, *Pis'ma, Zh. Eksp. Teor. Fiz.* **58**, 127 (1993) [*JETP Lett.* **58**, 131 (1993)].
- ⁷⁵Y. Kohori *et al.*, *J. Phys. Soc. Jpn.* **56**, 2263 (1987).
- ⁷⁶C. Stassis *et al.*, *Phys. Rev. B* **34**, 4382 (1986).
- ⁷⁷B. S. Shivaram, T. F. Rosenbaum, and D. G. Hinks, *Phys. Rev. Lett.* **57**, 1259 (1986).
- ⁷⁸P. A. Lee, T. M. Rice, J. W. Serene, L. J. Sham, and J. W. Wilkins, *Comments Condens. Matter Phys.* **12**, 99 (1986).
- ⁷⁹D. Fay and J. Appel, *Phys. Rev. B* **16**, 2325 (1977).
- ⁸⁰G. R. Stewart, *Rev. Mod. Phys.* **56**, 755 (1984).
- ⁸¹M. R. Norman, T. Oguchi, and A. J. Freeman, *Phys. Rev. B* **38**, 11 193 (1988).
- ⁸²D. W. Hess, T. A. Tokuyasu, and J. A. Sauls, *J. Condens. Matter Phys.* **1**, 8135 (1989).
- ⁸³C. H. H. Van Deurzen, K. Rajnak, and J. G. Conway, *J. Opt. Soc. Am. B* **1**, 45 (1984).